

Article

Experimental Investigation and Mechanism of Fly Ash/Slag-Based Geopolymer-Stabilized Soft Soil

Dazhi Wu , Zilong Zhang , Keyu Chen  and Linling Xia

School of Civil Engineering and Architecture, Zhejiang Sci-Tech University, Hangzhou 300018, China; 202030702059@mails.zstu.edu.cn (Z.Z.); chenkeyu0209@163.com (K.C.); 13588745299@163.com (L.X.)

* Correspondence: wudz@zstu.edu.cn; Tel.: +86-135-8873-8075

Abstract: In response to the high carbon emissions and energy consumption of traditional cement curing agents, in this paper, we propose a fly ash/slag-based geopolymer as an alternative to cement for stabilizing soft soils. In this study, the effects of the activator modulus, activator, and slag content on the geopolymer-stabilized clay were investigated by unconfined compressive strength (UCS) tests on Hangzhou soft soils, and the water stability and resistance to wet–dry cycles of the geopolymer-stabilized soils were studied. The changes in the microstructure and mineral phases were investigated using X-ray diffraction and scanning electron microscopy, respectively, and the inner evolution of the properties of the stabilized soft soil under different conditions was clarified. The test results revealed that the UCS of the geopolymer-stabilized soft soils increased and then decreased as the content and modulus of the alkali activator increased. The optimum mix proportion of geopolymer-stabilized soil required a modulus of the alkali activator of 0.6, a content of the alkali activator of 6%, and a slag-to-fly ash ratio of 1:1. Its 28-day UCS of the test specimens reached 2 MPa. When the content of the geopolymer was 25%, the water stability coefficient reached 87.53%, and the strength was still 1.6 MPa after eight wet–dry cycles. Based on the microscopic analysis, the cementing substances in the geopolymer-stabilized clay were calcium silicate hydrate (C-S-H) and sodium aluminosilicate hydrate (N-A-S-H), which made the soil's structure denser through bonding and filling effects.



Citation: Wu, D.; Zhang, Z.; Chen, K.; Xia, L. Experimental Investigation and Mechanism of Fly Ash/Slag-Based Geopolymer-Stabilized Soft Soil. *Appl. Sci.* **2022**, *12*, 7438. <https://doi.org/10.3390/app12157438>

Academic Editor: Daniel Dias

Received: 24 June 2022

Accepted: 20 July 2022

Published: 25 July 2022

Publisher's Note: MDPI stays neutral with regard to jurisdictional claims in published maps and institutional affiliations.



Copyright: © 2022 by the authors. Licensee MDPI, Basel, Switzerland. This article is an open access article distributed under the terms and conditions of the Creative Commons Attribution (CC BY) license (<https://creativecommons.org/licenses/by/4.0/>).

Keywords: fly ash/slag-based geopolymer; soft soil; stabilizer; experimental investigations; mechanistic analysis

1. Introduction

With the increasing population in coastal areas, the demand for infrastructure construction is also increasing; however, because the soft coastal soil has a high water content, high compressibility, low strength, poor stability, low bearing capacity, and other disadvantageous characteristics, it is difficult to directly carry out construction, and artificial solidification of soft ground is often needed to meet construction requirements [1]. Of the current soft soil treatments, deep soil mixing is one of the most commonly used treatment methods in China and abroad. In this treatment method, the physical and chemical interactions between the curing agent and the soft soil lead to the cured soil column having strength, integrity, and good water stability. Cement is often used as a soil-curing agent in engineering. This process mainly relies on cement hydrolysis and hydration reactions, and the action of the clay particles and cement hydrate to enhance the strength of the cement–soil mixture [2,3]. However, the cement production process is characterized by excessive energy and resource consumption, high CO₂ emissions, and serious pollution. In addition, it has a poor soft soil curing effect for soils with a high organic matter content and high plasticity index [4]. As a result, it imposes a huge burden on the environment. Therefore, it is of great engineering and environmental importance to identify new soft soil curing agents that are greener and more economically feasible.

Geopolymers are environmentally friendly cementitious materials formed from solid waste, natural minerals, artificial compounds, and other silica-aluminum-rich materials

through an activation reaction. Also known as green cement, the role of the activator is to dissolve the aluminum (Al) and silicon (Si) present in the precursor, forming an aluminosilicate gel [5]. With their high strength, low energy consumption, low cost, good volume stability, good impermeability, and chemical resistance, geopolymers are gaining wide attention and are being used in research applications worldwide [5–7]. In recent years, geopolymers have become more widely used in the concrete field and in stabilizing the pavement base, and the application of geopolymers to strengthen deep soft soils has gradually attracted the attention of scholars. The addition of a geopolymer has been found to increase the peak strength of treated soil and decrease the corresponding axial strain failure, both of which contribute to obtaining a stiff response similar to that of ordinary Portland cement (OPC)-stabilized soils [8,9]. Deng et al. [10] studied the effect of a geopolymer on the mechanical strength of cement-stabilized soil using test methods such as UCS, scanning electron microscopy (SEM), and mercury intrusion tests; they explored the mechanism by which it improved the strength of the cement-stabilized soil and verified the practicality and economy of using the geopolymer in cement soil based on field tests. Ye et al. [11,12] used water glass as the excitation agent of metakaolin in soft ground curing tests and selected the optimal combination based on the compressive strength and permeability data from the tests conducted on the use of cement and water glass excitation of metakaolin to stabilize soft soils. Pourakbar [13] used palm oil ash and fly ash-based polymers to stabilize sand and clay soils and investigated the long-term development pattern of the strength of the stabilized soils. Wang et al. [14] used an alkali-excited low-calcium fly ash cementitious material to stabilize silt soil and determined the trait evolution and microscopic mechanism of the strength of the alkali-excited fly-ash-stabilized silt by analyzing the macro- and microscopic properties, including compressive strength, chemical composition, cross-sectional morphology, and pore structure. Wu et al. [15] studied fly ash/slag-based geopolymer-stabilized silty clay and found that the pre-strength of the stabilized soil decreased with increasing fly ash content. It has been shown [16,17] that pure fly-ash-based geopolymer-reinforced soft soils require a longer maintenance time than cement to achieve the target strength, and fly ash is much less effective than cement when used alone or with slag for soft soil reinforcement. In engineering, due to environmental factors such as extreme weather and changes in the groundwater level, application of a curing agent often leads to changes in the strength characteristics of the stabilized soil. In-depth and systematic studies of the durability of stabilized soils such as cement have been carried out by domestic and foreign scholars [18,19].

The abovementioned research has focused on studying the UCS of geopolymer-stabilized soil, but few studies have been conducted on the water stability and resistance to wet–dry cycles of stabilized soil [20]. In our previous studies, we investigated the properties of a geopolymer and the application of the geopolymer to pavement repair and soft soil reinforcement [21–23]. Our research revealed that slag can promote the curing of a geopolymer at room temperature. Due to the presence of more calcium in slag, the early strength of a low-calcium activation has not been studied in-depth in relation to geopolymer-stabilized soils. Therefore, in this study, the effects of the slag replacement ratio and the alkalinity of the activator on the UCS of fly-ash-based geopolymer-stabilized soils were investigated by a single factor test and orthogonal test in addition to the water stability and resistance to wet–dry cycles of the geopolymer-stabilized soils. We also investigated its strength development pattern and effect on the stabilized soft soils and explored its microstructure and mechanism in order to explore the application of a fly-ash-based geopolymer, i.e., a low-carbon sustainable material, to replace cement in improving the properties of soft soil.

2. Experimental Work

2.1. Materials

The test soil was obtained from a foundation pit in the West Lake District, Hangzhou, China, and the soil was a typical silty soft clay. The basic physical properties of the soil are presented in Table 1. The fineness of the fly ash (FA) was 0.025 mm, and the specific surface

area of the ground granulated blast-furnace slag was 428 m/kg. Table 2 shows the main chemical components of GGBFS and FA. FA and slag are potentially reactive materials, and their hydration process is accelerated by chemical excitation. Since the total content of Al_2O_3 , SiO_2 , and Fe_2O_3 (85.26%) in FA is greater than 70%, and the content of CaO is less than 10%, the classification standard of the American Society for Testing and Materials (ASTM) (2015) classifies FA as class F material. For the slag, CaO is dominant, followed by Al_2O_3 and SiO_2 . The water glass used was commercially available liquid water glass with an initial modulus of 3.30 and a solid content of 34.8%. The NaOH used was a solid flake form with an analytical purity of greater than 99% produced by the Wuxi Yatai United Chemical Co. (Wuxi, China).

Table 1. Basic physical properties of Hangzhou soil specimens.

Liquid Limit	Plastic Limit	Natural Moisture Content	Relative Density	Clay	Silt	Sand
36.20%	23.45%	45.86%	2.68	28%	59%	13%

Table 2. Chemical composition of FA and GGBFS (%).

Material	Al_2O_3	SiO_2	Fe_2O_3	CaO	MgO	Others
Fly ash	23.67	56.96	4.63	1.50	1.50	13.24
GGBFS	16.32	36.10	1.28	35.58	6.54	4.18

2.2. Testing Procedures

To obtain a uniform soil structure, geopolymer-stabilized soil specimens were prepared according to the following procedure. The collected soft soil was dried on site at a low temperature (50–60 °C), crushed using a pulverizer, and passed through a 2-mm sieve. The corresponding masses of dry soil, fly ash, and slag were mixed well. Then, the corresponding masses of water and the compound activator solution (which had been left to stand for 24 h) were added, and the mixture was stirred again until it reached a homogeneous state. According to Chinese standard JGJ/T 233-2011 [24], the soil mixture was poured into a $70.7 \times 70.7 \times 70.7 \text{ mm}^3$ cubic mold in three stages, and the air bubbles in the specimens were eliminated by vibrating each layer for 2 min. The soil specimens were sealed into the standard curing box (temperature of $20 \pm 2 \text{ °C}$, relative humidity of >95%), stabilized for 24 h, and then demolded. After curing for one day, the soil specimens were demolded and sealed in plastic wrap and then placed into the curing box until the tests were performed.

The UCS of the specimen was measured using a WAW-300B electromechanical universal testing machine with a maximum force of 30 kN, and the loading rate was set to 1 mm/min. The average value of the strengths of the three specimens was taken as the representative strength. Selected internal fragments of typical specimens after strength testing were dried at low temperature in an oven at 50 °C, ground, and passed through a 0.075-mm sieve for XRD analysis. The mineralogical changes were determined using a D8 Advance XRD, with 2θ of 10–80° and a scanning speed of 0.5 s. Small specimens with fresh natural surfaces inside were selected for SEM analysis. The fresh surfaces were not touched or polished to avoid affecting the observations. The microstructures of the gold-sprayed fracture surfaces of the specimen (without polishing) were observed using a Gemini 500 field emission scanning electron microscope (FESEM), with an accelerated voltage of 3 kV. Using nitrogen as the adsorbate, the nitrogen adsorption and desorption tests were carried out at 90 °C, and the adsorption and desorption times were 12 h. The pore diameter distribution was analyzed by the BJH method dV/dD through the adsorption–desorption curve.

2.3. Preparation of Specimens

The initial moisture content of the soil used in the tests was 50% (the ratio of the moisture to the dry soil mass). The content of the geopolymer (ratio of the sum of FA and

slag to the mass of dry soil) was 20%. The water–binder ratio of the geopolymer was 0.3, the alkali activator content and modulus were 7% and 1, respectively, and the setting times of different slag contents are shown in Table 3. The effects of the slag content (mass ratio of slag to precursors), alkali activator modulus (the molar ratio of SiO_2 to Na_2O in the alkali activator), and alkali activator content (ratio of alkali activator to dry soil mass) on the geopolymer-stabilized soil were investigated. The specific mixture proportions are presented in Table 4. We designed a three-factor and three-level orthogonal experiment to explore the optimal mix ratio, as shown in Table 5. The optimal polymer mix ratio was used in the water stability test; the geopolymer contents were 10%, 15%, 20%, and 25%. According to the relevant testing specifications [25], the specimens were soaked in water for 32 d after 28 d of standard maintenance. Then, the UCS of the specimens were measured after wiping them dry, and the strengths of the specimens were compared with that of the unsoaked specimens in order to determine the water stability of the geopolymer-stabilized soft soils. Wet–dry cycle test specimens were prepared using the same ratio as that used for the water stability test, and the following steps were performed after 28 days of standard maintenance [26]. The specimen was heated in the oven at 50 °C for 24 h, removed from the oven, and placed at room temperature for 1 h to cool. Then, it was placed in water and soaked for 23 h, which completed a wet–dry cycle. In the wet–dry cycle tests, the strengths of specimens that had undergone 0, 2, 4, 6, and 8 wet–dry cycles were tested and compared with the standard curing strengths of the corresponding ages.

Table 3. Setting time of different slag content.

Slag Content	Initial Setting Time/min	Final Setting Time/min
0%	156	354
10%	101	268
30%	64	127
50%	48	65

Table 4. Testing schemes.

Slag Replacement Ratio (%)	Modulus of Activator	Activator Content (%)	Dry Soil (g)	NaOH (g)	Na_2SiO_3 (g)	FA (g)	Slag (g)
10	1.0	7	800	11.06	44.94	144	16
30	1.0	7	800	11.06	44.94	112	48
50	1.0	7	800	11.06	44.94	80	80
70	1.0	7	800	11.06	44.94	48	112
90	1.0	7	800	11.06	44.94	16	144
30	0.6	7	800	18.21	37.79	112	48
30	0.8	7	800	14.04	41.97	112	48
30	1.0	7	800	11.06	44.94	112	48
30	1.2	7	800	8.84	47.16	112	48
30	1.0	5	800	7.90	32.10	112	48
30	1.0	6	800	9.48	38.52	112	48
30	1.0	7	800	11.06	44.94	112	48
30	1.0	8	800	12.64	51.36	112	48
30	1.0	9	800	14.22	57.78	112	48

Table 5. Orthogonal test factor and level table.

Influencing Factors	Level 1	Level 2	Level 3
activator modulus (A)	0.6	0.8	1.0
activator contents (B)	5%	6%	7%
slag content (C)	10%	30%	50%

3. Response Surface Analysis

3.1. UCS of Geopolymer-Stabilized Soft Soils

3.1.1. Effect of Slag on UCS of Stabilized Soil

The variations in the UCS of the stabilized soil with the curing age after the addition of different proportions of blast furnace slag are shown in Figure 1. It can be seen that the strength of the geopolymer-stabilized soil gradually increased with age. When the slag content was increased from 10% to 50%, the UCS of the geopolymer solidified soil increased slightly. When the content was 50%, the strength of the solidified soil cured for 28 d was 1.53 MPa. When the slag content was increased from 50% to 90%, the UCS of the stabilized soil increased dramatically, reaching 7.20 MPa at 90%. This shows that the excitation effect of the alkali activator on slag was significantly stronger than that of the FA, and the excitation of the slag played a major role in the increase in the strength of the stabilized soil specimens [27]. The reason for this is that the slag contained more vitreous than the FA, and the SiO_4^{4-} in the vitreous was easily depolymerized and hydrated by the other substances under the alkaline environment. In addition, the CaO content of the slag was several times higher than that of the FA. The Si and Al ions polymerized with Ca^{2+} and formed a large number of overlapping gel products, which were beneficial to the strength development of the stabilized soil [28].

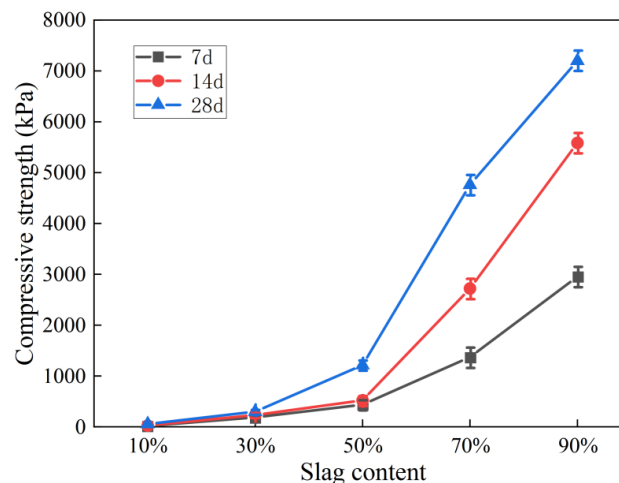


Figure 1. UCS of stabilized soils with different slag contents.

3.1.2. Effect of Alkaline Activator Modulus on UCS of Stabilized Soil

The alkali activator modulus is the molar ratio of SiO_2 to Na_2O , and it is one of the important parameters of a geopolymer alkali activator. Figure 2 shows the variations in the UCS of the geopolymer-stabilized soil when the modulus of the geopolymer alkaline activator increased from 0.6 to 1.0 with a 7% alkali activator content. As the modulus increased, the UCS of the stabilized soil initially increased and then decreased, and the UCS of the stabilized soil reached the maximum when the modulus was 0.8. These results indicate that for FA-based geopolymer-stabilized soils, the optimum modulus is 0.8, and a higher modulus weakens the alkalinity and reduces the dissolution rate of the geopolymer silica-alumina materials (FA and slag), which affects the strength of the stabilized soil. OH^- will react with the metal cations during the clay reaction, destroying the soil's structure and inhibiting the growth of the gel phase material, thus leading to a reduction in the strength of the stabilized soil [29]. When the modulus is less than 0.8, the alkalinity of the material is too strong, the content of the active $[\text{SiO}_4^{4-}]$ in the reaction is reduced, and the OH^- reacts with the metal cations in the clay, destroying the soil's structure and inhibiting the growth of the gel phase substances. This results in a decrease in the strength of the stabilized soil.

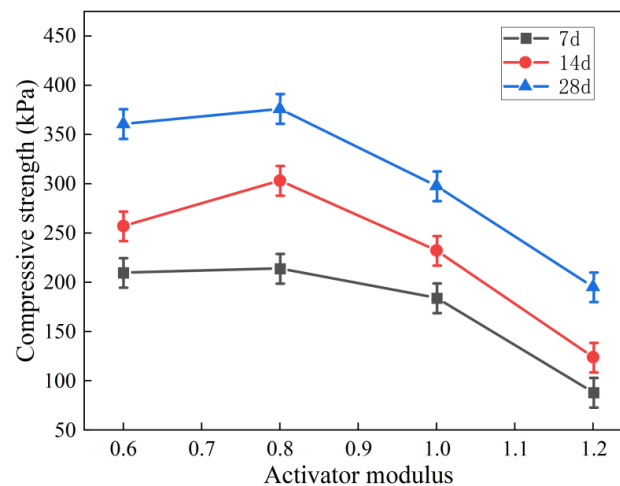


Figure 2. UCS of stabilized soils with different alkali activator modulus.

3.1.3. Effect of Alkaline Activator Content on UCS of Stabilized Soil

Figure 3 shows the compressive strength variations in the fly-ash-based geopolymer-stabilized soils with alkali activator content (modulus of 1.0 and a slag content of 30%). As can be seen from Figure 3, the UCS of the stabilized soil did not always increase with increasing alkali activator content, and it reached the highest value when the alkali activator content was 6%, after which the strength of the geopolymer-stabilized soil decreased with increasing alkali activator content. The increased OH^- in the system led to excessive early deposition of the silicate products, which hindered the later reaction of the Si and Al [30]. However, when the activator content was too high, the excessive amount of alkali metal ions M^+ affected the charge balance of the system, which was not conducive to the formation and development of the structure [31]. When the hydration reaction occurred for a certain amount of time, the reaction products could only cover the surface of the structure, which hindered the contact between the geopolymer and the soft soil, resulting in excessive alkaline activator residue, which was not conducive to the development of the overall structure of the solidified soil.

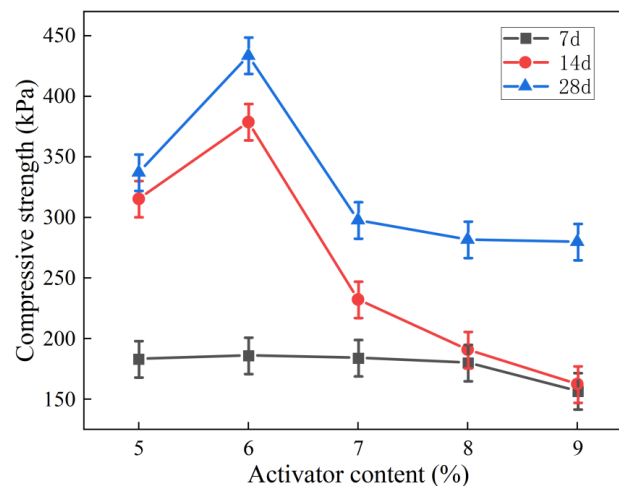


Figure 3. UCS of stabilized soils with different alkali activator contents.

3.2. Analysis of Orthogonal Pressure Resistance Results

Table 6 shows that the influence order of each control factor on the 7-day and 28-day geopolymer stabilized soil is consistent, which is: $C > A > B$. This indicates that the geopolymer material is relatively stable. In the process of reinforcing soft soil, with the increase of age, the main influencing factors are the compressive strength of the geopolymer-

stabilized soil. The degree of impact will not change. The optimal ratio of compressive strength of 7 days and 28 days is the same: A1, B2 and C3, that is, the activator modulus is 0.6, the alkali activator content is 6%, and the slag content is 50%.

Table 6. Orthogonal test analysis table.

Test Number	A	B	C	UCS/kPa	
				7 d	28 d
1	1	1	1	41.05	127.5
2	2	2	2	224.47	396.1
3	3	3	3	437.33	1214.8
4	1	2	3	920.68	2000
5	2	3	1	33.79	66.4
6	3	1	2	183.27	337.4
7	1	3	2	209.81	360.71
8	2	1	3	493.95	1509.9
9	3	2	1	18.98	39.8
K1	1171.54	718.27	93.82	7-day Compressive strength	
K2	752.21	1164.13	617.55		
K3	639.58	680.93	1851.96		
k1	390.51	239.42	31.27		
k2	250.74	388.04	205.85		
k3	213.19	226.98	617.32		
R (range)	531.96	483.2	1758.14		
K1	2488.21	1974.80	233.70	28-day Compressive strength	
K2	1972.40	2435.90	1094.21		
K3	1592.00	1641.91	4724.70		
k1	829.40	658.27	77.90		
k2	657.47	811.97	364.74		
k3	530.67	547.30	1574.90		
R (range)	896.21	793.99	4491.00		

3.3. Compared with the Mechanical Properties of Cement-Stabilized Soil

Under the same conditions, take 20% geopolymers- and cement-stabilized soft soil, respectively. The cement is P.O. 42.5 ordinary Portland cement with a water–cement ratio of 0.5. The mix ratio of geopolymer stabilized soil is the best mix ratio of the above orthogonal test. A comparative analysis of the effect of geopolymer and cement in strengthening soft soil was conducted. Figure 4 is a comparison chart of the compressive strength of cement-soil test block and geopolymer-soil test block at different ages. It can be seen that the unconfined compressive strength of cement-soil and geopolymer soil increases with the increase of curing time. Under the same conditions, the compressive strength of cement-stabilized soft soil is higher than that of fly-ash-slag based geopolymer stabilized soft soil. From 0 to 28 days, the compressive strength of cement-soil increased rapidly, and its strength reached 2.87 MPa at 28 days. However, from 28 to 90 days, the growth rate of the compressive strength of cement-soil slowed down, which was lower than the growth rate of geopolymer-stabilized soil [32]. The geopolymer-stabilized soil reached 3.21 MPa at 90 d.

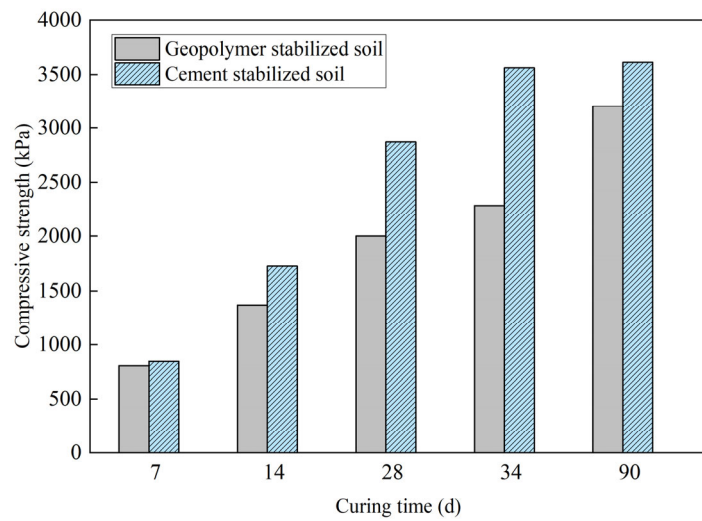


Figure 4. Compressive strength of the soil stabilized by geopolymer and OPC.

It can be seen from Figure 5 that the cohesion of the cement-stabilized soil is greater than that of the geopolymer-stabilized soil, and the internal friction angle of the cement-stabilized soil is smaller than that of the geopolymer-stabilized soil. It can be seen that both cement and geopolymer can significantly improve the compressive and shear strength of soft soil and can play a good role in improving the mechanical properties of soft soil. It can far meet the strength requirements of mixing piles in practical projects.

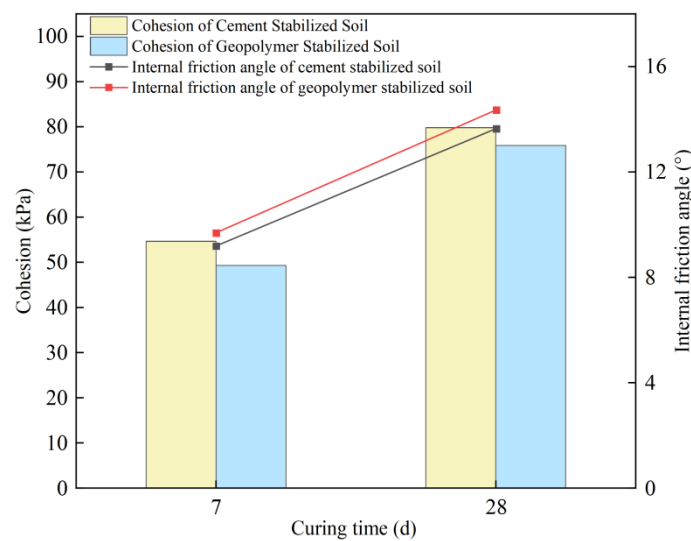


Figure 5. Shear resistance of the soil stabilized by geopolymer and OPC.

3.4. Stability Study of Geopolymer Stabilized Soft Soil

3.4.1. Water Stability Studies

The water stability coefficient (Equation (1)) was used to evaluate the water stability of the geopolymer-stabilized soil in the water stability test [25].

$$\delta_{cT} = \frac{R_{cRT}}{R_{cT}} \times 100\% \tag{1}$$

where δ_{cT} is the water stability coefficient and R_{cRT} and R_{cT} are the UCS (kPa) of the soaked and unsoaked samples at age T, respectively.

The soft soil without geopolymer could not be shaped, and when the soft soil was mixed with geopolymer, the sample was still intact after 32 days of complete water im-

mersion, reflecting that the stabilization of the soft soil using the geopolymer significantly improved the water stability of the soft soil. The main reason for the improvement of the water stability of the geopolymer-stabilized soft soils was that the gelling substances generated by the geopolymerization reaction bound the soil particles to each other and filled the pores of the soil particles effectively, thus forming a spatial mesh skeleton structure, which enhanced the stability and overall structure of the stabilized soil [20].

The UCS of the specimens before and after water immersion were the most direct indicator of the water stability of the geopolymer-stabilized soft soils. Figure 6 shows the UCS and water stability coefficients of the geopolymer-stabilized soft soils with geopolymer contents of 10%, 15%, 20%, and 25% under standard maintenance and continuous water immersion for 32 days. It can be seen that the water stability coefficients were all greater than 80%, which reflects the water stability of the geopolymer-reinforced soils. The comparison shows that the softening effect of the water immersion reduced the UCS of the geopolymer-stabilized soil. When the geopolymer content was higher, the loss rate of compressive strength was lower, and the water stability was higher. This is because the more geopolymer was incorporated, the more gel material was generated by the action of the geopolymer, which increased the bonding effect and strengthened the overall structure of the stabilized soil, thus increasing its ability to resist the weakening effect of the water immersion.

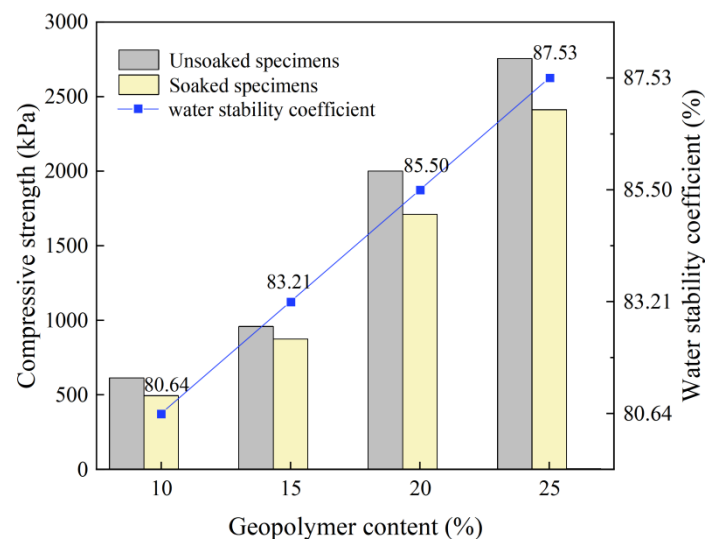


Figure 6. UCS of unsoaked and soaked geopolymer-stabilized soil.

3.4.2. Wet–Dry Cycle Tests on Geopolymer-Stabilized Soft Soils

Figure 7 shows the change in the appearance of the geopolymer-stabilized silty soft soil with a geopolymer content of 10% under different numbers of wet–dry cycles. For the specimen with a 10% geopolymer content, there was obvious peeling of the outer skin on the surface of the specimen after one wet–dry cycle, serious damage after two to four cycles, and almost all of the outer layer of the specimen peeled off after the fourth cycle. The specimen exhibited local collapse and cracks at the end of the sixth cycle. The specimens with a 15% geopolymer content started to develop minor cracks and small pieces peeled off after the fourth wet–dry cycle. In contrast, for the specimens with geopolymer contents of 20% and 25%, the surfaces were almost completely intact after six wet–dry cycles. The above phenomenon demonstrates that a proper increase in the geopolymer content of stabilized soil will provide better resistance to damage caused by wet–dry cycles.

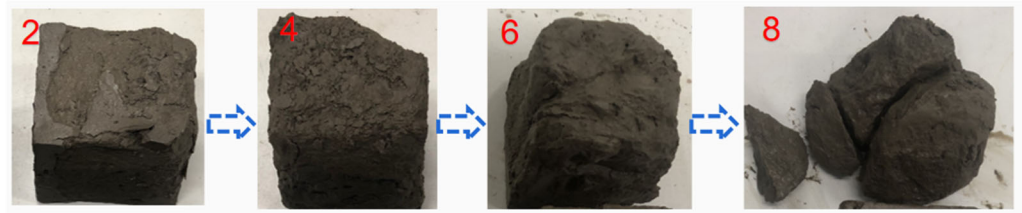


Figure 7. Appearance changes of specimens with 10% geopolymer content in wet–dry cycles. The number of cycles is 2, 4, 6, 8.

The variations in the strengths of the stabilized soils with different geopolymer contents with an increasing number of wet–dry cycles are shown in Figures 8 and 9. The bottom horizontal axis of the graph is the number of wet–dry cycles, and the top horizontal axis is the time of standard maintenance of the stabilized soil corresponding to the number of cycles. The strengths of the standard stabilized specimens exhibit an overall increase with increasing age, but the lower the geopolymer content of the stabilized soil is, the smaller the increase is. Under the wet–dry cycles conditions, the specimens with different geopolymer contents exhibited a trend of gradually decreasing strength with an increasing number of wet–dry cycles, and the strengths of the specimens under the wet–dry cycles were lower than their corresponding standard curing strengths. This is because in the process of the wet–dry cycles, the internal structure of the specimens is damaged due to the dry shrinkage and wet expansion processes, especially the formation of cracks at the bonding weakness points between the soil particles [19]. As the number of cycles increased, the specimens continued to shrink and expand in the dry and wet phases of the cycles, respectively, which led to larger cracks forming until damage occurred. The strength of the sample containing 20% ground polymer at the end of eight cycles was 982.16 kPa, that is, a strength loss of 51% compared to that under zero cycles. However, the strength of the specimen with continued standard curing was 2439.84 kPa, which was much higher than that of the dry–wet cycle specimens. As the geopolymer content increased, the strength of the specimens after eight cycles increased, and the strength losses of the stabilized soil with 10%, 15%, 20%, and 25% geopolymer contents were 100%, 67%, 51%, and 42%, respectively. This also indicates that increasing the geopolymer content can effectively reduce the strength loss and enhance the performance of the stabilized soft soil against wet–dry cycles.

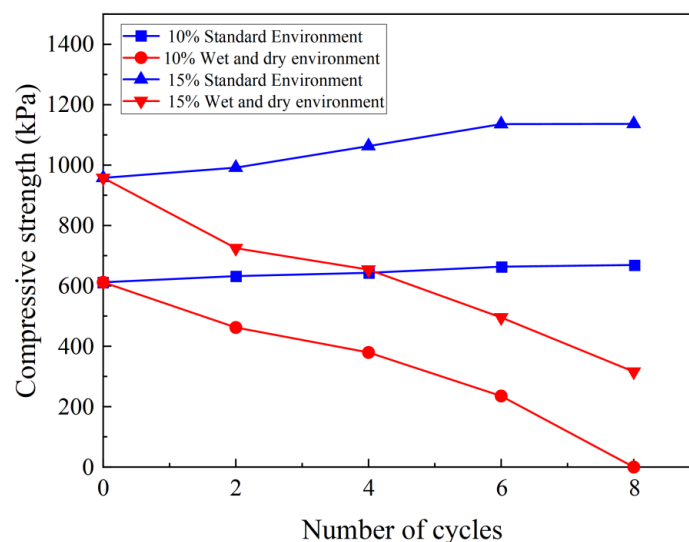


Figure 8. Variations in the compressive strengths of the samples with curing agent contents of 10% and 15% with an increasing number of wet–dry cycles.

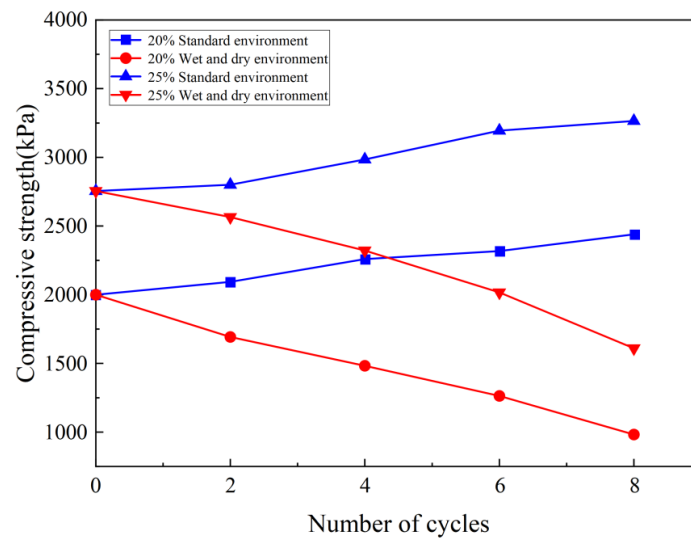


Figure 9. Variations in the compressive strengths of the samples with curing agent contents of 20% and 25% with an increasing number of wet–dry cycles.

3.5. Mechanistic Analysis of Geopolymer-Stabilized Soft Soil

3.5.1. Component Analysis

XRD was used to analyze the physical phases of the geopolymer-stabilized soils to determine the hydration products formed when the geopolymer stabilized the soft soils. XRD analysis was carried out on the undisturbed soil and typical samples with curing ages of 28 days (Figure 10). Figure 10 shows that there are two main types of phases in Hangzhou soft soil: a clay phase and a crystalline phase. The clay phase was mainly composed of montmorillonite, and the second crystalline phase was mainly composed of quartz and albite. The XRD analysis of the geopolymer-stabilized soft soils revealed that they contained two types of phases. The crystalline phase was basically consistent with that of the soft soil, and no new minerals were produced during the process by which the geopolymer stabilized the soft soil.

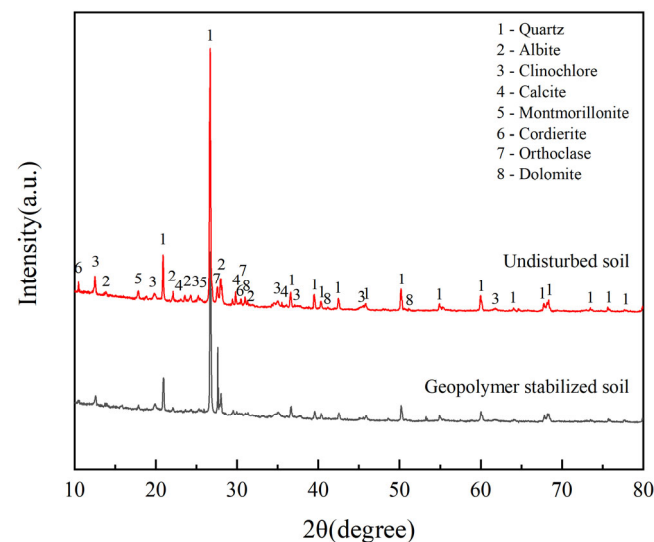


Figure 10. XRD patterns of undisturbed soil and geopolymer-stabilized soil.

Based on the position of each diffraction peak, the amount of crystalline phase increased, and quartz and albite were clearly visible in the geopolymer soil compared with the undisturbed soil. In the $2\theta < 45^\circ$ region of the XRD spectra, there are amorphous continuous diffuse peak packets, which indicate that the hydration and alkaline activator

reactions of the FA, slag, and activator in the soft soils under the action of the water medium generated the amorphous phases. Calcium (alumo)silicate hydrate C-(A)-S-H and sodium aluminosilicate hydrate (N-A-S-H) were two of the main products of the geopolymerization reaction [12]. This is due to the potential active components within the silica-alumina in the raw geopolymer materials (slag and FA), which can be sufficiently excited by the alkaline activator, causing the Si-O and Al-O bonds to break and re-polymerize to generate these two main products [11].

3.5.2. Microstructural Observations

The morphology of the hydration products, the microscopic morphology, and the pore structure of the geopolymer-stabilized soft soils were observed via SEM. Figure 11 presents the SEM images of the FA, slag, and undisturbed soil. As can be seen from Figure 11, the FA particles are spherical and the slag particles are angular with irregular shapes and sharp edges. The scaly clay minerals in the soft soil exhibit obvious edge–edge structures, and the particles are not compactly connected and have more pores, which is the reason for the poor mechanical properties of the undisturbed soil. Figure 12b,c show that the addition of the geopolymer significantly improved the soil's structure, and the particles became more tightly connected and less porous compared to the original soil. In addition, numerous white needle-like and flocculent cementation products can be seen attached to the soil particles. The flocculent white gelling products are mainly the C-S-H and N-A-S-H gelling substances generated from the SiO_2 and Al_2O_3 in FA and slag through reactions with the compound activator [33–35]. These products wrap the soil particles and make the soil denser, reducing its porosity. In addition, the ettringite needle-like hydration products can be seen in the SEM image of the geopolymer soil. The main reason why ettringite could have grown in large quantities is that the soil particles were relatively loose.

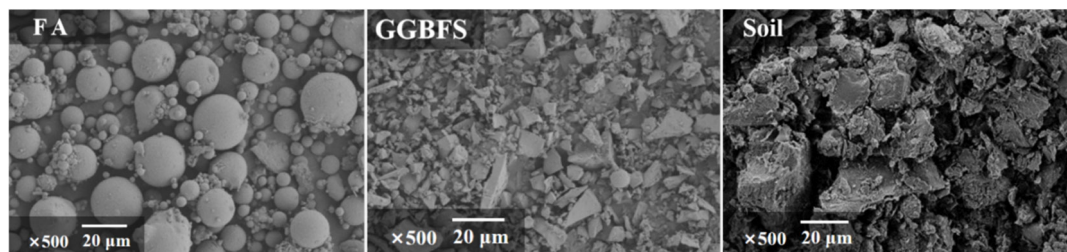


Figure 11. SEM images of the FA, slag (GGBFS), and undisturbed soft soil.

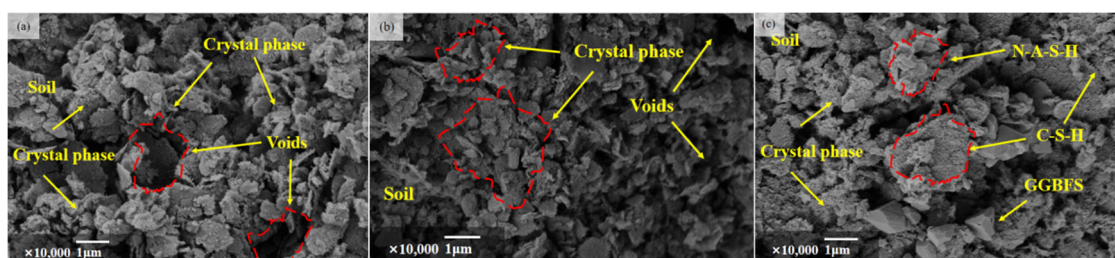


Figure 12. Electron microscope scans of the soft soil stabilized using different mixture ratios. (a) Activator modulus = 0.8, alkali content = 7%, slag = 30% geopolymer soil, (b) activator modulus = 1.0, alkali content = 7%, slag content = 30% ground polymer soil, and (c) activator modulus = 0.6, alkali content = 6%, slag = 50% geopolymer soil.

Figure 12a,b present the SEM images of the geopolymer soil specimens with activator moduli of 0.8 and 1.0, respectively. The geopolymer soil specimen with a modulus of 0.8 is more dense and less porous than that with a modulus of 1.0, and the surfaces of the soil particles are covered with more white colloidal material. A large amount of white colloidal hydration products can be seen in Figure 12a, which indicates that a modulus of

0.8 provides a suitable alkaline environment for the geopolymer reaction to occur to a more adequate extent, producing more colloidal products that effectively fill the spaces between the soil particles. Figure 12a,c present the SEM images of the geopolymer soil specimens with slag contents of 30% and 50%, respectively. More unreacted slag particles can be seen in Figure 12c, which shows that the geopolymer-stabilized soil particles become more closely connected and the pore space gradually decreases with increasing slag content [15]. This is due to the fact that the slag provides more Ca^{2+} to participate in the geopolymerization reaction, which generates more C-S-H and N-A-S-H, while the exotherm of the slag in the hydration reaction promotes the geopolymerization reaction [22,34].

3.5.3. Pore Structure Analysis

MxCySz is used to represent activator modulus = x , alkali content = $y\%$, slag content = $z\%$. Figure 13 shows the pore diameter distribution of geopolymer-stabilized soft soils with different mix ratios. At the pore diameter 4–5 nm, the pore volume is the largest, indicating that the internal pore diameter of the sample is mainly 4–5 nm. The samples of the activator modulus of 0.8 and 1 were compared. It can be seen that the pore volume of the activator modulus of 0.8 is relatively large when the pore diameter is less than 4 nm; when the pore diameter is greater than 5 nm, the pore volume of the activator modulus of 1 is relatively large, which indicates that the sample of activator modulus of 0.8 contains more pores less than 4 nm and the structure is more compact. The pore volume of the small pores with the optimal component is the largest, the structure is stable, and the intensity is the highest. It is precisely because the geological polymer bonds the soil particles and improves the contact method between the soil particles as well as filling the pores between the soil particles, reducing the internal pores and thereby making the soil structure firm [23].

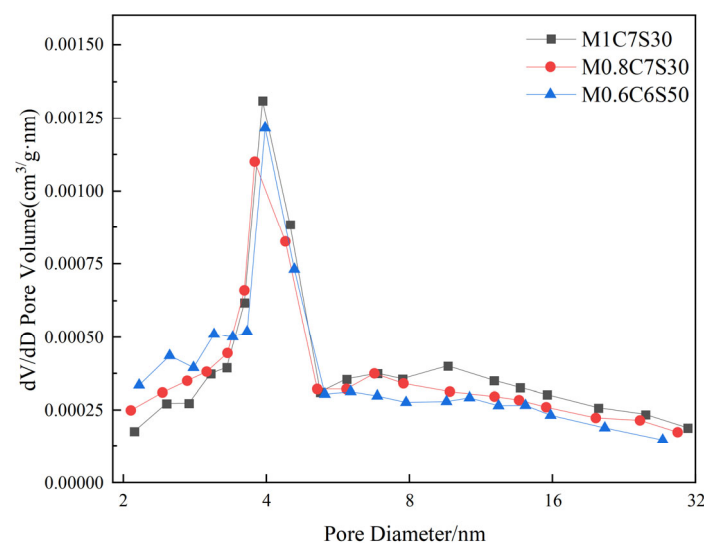


Figure 13. Pore diameter distribution of the soft soil stabilized using different mixture ratios.

3.6. Carbon Emissions and Economic Analysis of the Geopolymer Stabilizer

After collecting the average prices of local suppliers, an economic analysis was carried out on the geopolymer stabilizer with the optimal mix ratio in this paper. The cost details are shown in Table 7. As can be seen from the table (ignoring the cost of water), the cost of silica-alumina raw materials for geopolymers (193.64) is much lower than that of cement, and the total cost of geopolymers is higher than that of cement. However, fly ash and slag are industrial wastes. If they are not used, the local waste treatment standard is 300 yuan/ton. Therefore, the overall economic benefits of geopolymers are still significant. From the cost analysis of geopolymers, it can be seen that the cost of alkali activators is relatively large. Some scholars [36] have proposed to reduce the degree of incorporation of alkaline solution. Wu et al. [37] proposed that the slag was activated by waste alkaline

water from a chemical company to prepare a geopolymer. This also shows that the cost of geopolymer still has great development potential.

Table 7. Assessment of the cost of two types of soft soil stabilizers.

Phase (yuan rmb/ton)	OPC	Geopolymer
Solid	P.O. 42.5: 500	FA: 32.27; GGBFS: 161.37; NaOH: 146.91
Liquid	Water: 0	Na ₂ SiO ₃ : 106.72; Water: 0
Total cost	300	447.27

Geopolymers enable the construction industry to meet the sustainability requirement and reduce the global impact (lower carbon cost). Compared with cement, geopolymer can reduce carbon emissions by 44–64% [38]. Different types of industrial wastes and maintenance methods will affect the carbon emissions of geopolymers, but alkali activators are the main source of carbon emissions from geopolymers, accounting for 20–65% of the total emissions [39,40]. In the future, choosing a low-carbon alkali activator and reducing the dosage will be an important avenue for further carbon reduction of geopolymers.

4. Conclusions

Soft soils were stabilized using a geopolymer, and the effects of the various factors on the stabilization of the soft soils were investigated through indoor tests. In addition, in-depth analysis of the water stability and resistance to wet–dry cycles of the stabilized soils was conducted. Microscopic analysis of the stabilized soils was carried out to reveal the principles and mechanisms corresponding to the macroscopic mechanical properties. Based on the results of this study, the following conclusions can be drawn.

- (1) The application of FA/slag-based geopolymer as a curing agent to stabilize soft soil can significantly improve the strength of the soil. When the geopolymer content was fixed, the slag, alkali activator content, and the modulus of the alkali activator had significant effects on the stabilization of the soil. The strength initially increased and then decreased as the content and modulus of the alkali activator increased. The optimum mix proportion of geopolymer-stabilized soil required a modulus of the alkali activator of 0.6, a content of the alkali activator of 6%, and a slag-to-fly ash ratio of 1:1.
- (2) An FA/slag-based geopolymer can effectively improve the water stability of silty soft soils. The geopolymer-stabilized soil test specimens were intact after water immersion, without any peeling or cracking phenomena, and the strengths of the soaked specimens were significantly lower than those of the test specimens without water immersion.
- (3) The incorporation of an FA/slag-based geopolymer significantly improved the resistance of the soft soils to wet–dry cycles. The loss of strength of the specimen decreased as the geopolymer content increased. The specimens with geopolymer contents of 20% and 25% exhibited almost no peeling of the outer skin after six cycles.
- (4) Based on microscopic analysis, the cementing substances in the geopolymer-stabilized soil mixture system were identified as C-S-H and N-A-S-H. The main mechanism by which the geopolymer reinforced the soft soil was as follows. Some of the FA and slag particles did not react with the compound activator, but their smaller particles effectively filled the large voids between the soil particle and reduced the porosity of the soil. The geopolymerization reaction produced a large number of gelling products, which encapsulated and bonded the soil particles, forming a denser structure and increasing the compressive strength of the stabilized soil.

Author Contributions: Conceptualization, D.W.; methodology, Z.Z.; software, K.C.; validation, Z.Z. and L.X.; formal analysis, Z.Z.; investigation, Z.Z.; resources, Z.Z.; data curation, L.X.; writing—original draft preparation, Z.Z.; writing—review and editing, Z.Z.; visualization, D.W. and Z.Z.;

supervision, D.W.; project administration, K.C.; funding acquisition, D.W. All authors have read and agreed to the published version of the manuscript.

Funding: This research was funded by the National Natural Science Foundation of China, grant number 51678533.

Institutional Review Board Statement: Not applicable.

Informed Consent Statement: Not applicable.

Data Availability Statement: Details on all data supporting the reported results can be obtained in Tables 1–7 and Figures 1–13, this original manuscript.

Conflicts of Interest: The authors declare no conflict of interest.

References

- Guo, Q.; Wei, M.L.; Wu, H.L.; Gu, Y.Z. Strength and micro-mechanism of MK-blended alkaline cement treated high plasticity clay. *Constr. Build. Mater.* **2020**, *236*, 117567. [[CrossRef](#)]
- Porbaha, A. State of the art in deep mixing technology: Part I. Basic concepts and overview. *Proc. Inst. Civ. Eng. Ground Improvement.* **1998**, *2*, 125–139. [[CrossRef](#)]
- Puppala, A.J.; Pedarla, A. Innovative ground improvement techniques for expansive soils. *Innov. Infrastruct. Solut.* **2017**, *2*, 01641468. [[CrossRef](#)]
- Hassan, A.; Arif, M.; Shariq, M. A review of properties and behaviour of reinforced geopolymer concrete structural elements—A clean technology option for sustainable development. *J. Clean Prod.* **2020**, *245*, 118762. [[CrossRef](#)]
- Luhar, S.; Luhar, I.; Nicolaides, D.; Gupta, R. Durability Performance Evaluation of Rubberized Geopolymer Concrete. *Sustainability* **2021**, *13*, 5969. [[CrossRef](#)]
- Saloni, Parveen; Pham, T.M.; Lim, Y.Y.; Malekzadeh, M. Effect of Pre-treatment Methods of Crumb Rubber on Strength, Permeability and Acid Attack Resistance of Rubberised Geopolymer Concrete. *J. Build. Eng.* **2021**, *41*, 102448. [[CrossRef](#)]
- Khan, S.I.; Abegaz, G.T.; Jaleta, B. A high-performance geopolymer concrete an experimental study using fly ash, GGBS and copper slag. *J. Struct. Eng. Madras* **2021**, *48*, 71–84.
- Abdullah, H.H.; Shahin, M.A.; Prabir, S. Use of Fly-Ash Geopolymer Incorporating Ground Granulated Slag for Stabilisation of Kaolin Clay Cured at Ambient Temperature. *Geotech. Geol. Eng.* **2019**, *37*, 721–740. [[CrossRef](#)]
- Rios, S.; Ramos, C.; Viana da Fonseca, A.; Cruz, N.; Rodrigues, C. Mechanical and durability properties of a soil stabilised with an alkali-activated cement. *Eur. J. Environ. Civ. Eng.* **2019**, *23*, 245–267. [[CrossRef](#)]
- Deng, Y.F.; Wu, Z.L.; Liu, S.Y.; Yue, X.B.; Guan, Y.F. Influence of geopolymer on strength of cement-stabilized soils and its mechanism. *Chin. J. Geotech. Eng.* **2016**, *38*, 446–453.
- Ye, H.Y.; Zhang, W.F.; Wei, W.; Dong, Y.L.; Zhang, W.Y. Experimental Study on the Curing of Soft Soil with Activator-Geopolymer. *J. Basic Sci. Eng.* **2019**, *27*, 906–917.
- Zhou, H.Y.; Wang, X.S.; Hu, X.X.; Xiong, Z.Q.; Zhang, X.Y. Influencing factors and mechanism analysis of strength development of geopolymer stabilized sludge. *Rock Soil Mech.* **2021**, *42*, 2089–2098. [[CrossRef](#)]
- Pourakbar, S.; Huat, B.B.; Asadi, A.; Fasihnikoutalab, M.H. Model study of alkali-activated waste binder for soil stabilization. *Int. J. Geosynth. Ground Eng.* **2016**, *2*, 35. [[CrossRef](#)]
- Wang, D.X.; Wang, H.W.; Zou, W.L.; Wang, X.Q.; Li, L.H. Research on micro-mechanisms of dredged sludge solidified with alkali-activated fly ash. *Chin. J. Rock Mech. Eng.* **2019**, *38* (Suppl. S1), 3197–3205. [[CrossRef](#)]
- Wu, J.; Zheng, X.Y.; Yang, A.W.; Li, Y.B. Experimental Study on the Compressive Strength of the One-Part Slag-fly Ash based Geopolymer Stabilized Muddy Clay. *Rock Soil Mech.* **2021**, *42*, 9.
- Rivera, J.F.; Orobio, A.; Cristelo, N.; Gutiérrez, R.M.D. Fly ash-based geopolymer as A4 type soil stabiliser. *Transp. Geotech.* **2020**, *25*, 100409. [[CrossRef](#)]
- Salimi, M.; Ghorbani, A. Mechanical and compressibility characteristics of a soft clay stabilized by slag-based mixtures and geopolymers. *Appl. Clay Sci.* **2020**, *184*, 105390. [[CrossRef](#)]
- Li, L.; Shao, W.; Li, Y.D.; Cetin, B. Effects of Climatic Factors on Mechanical Properties of Cement and Fiber Reinforced Clays. *Geotech. Geol. Eng.* **2015**, *33*, 537–548. [[CrossRef](#)]
- Zha, F.S.; Liu, J.-J.; Xu, L.; Cui, K.-R. Cyclic wetting and drying tests on heavy metal contaminated soils solidified/stabilized by cement. *Chin. J. Geotech. Eng.* **2013**, *35*, 1246–1252.
- Chowdary, V.B.; Ramanamurty, V.; Pillai, R.J. Experimental evaluation of strength and durability characteristics of geopolymer stabilised soft soil for deep mixing applications. *Innov. Infrastruct. Solut.* **2021**, *6*, 40. [[CrossRef](#)]
- Chen, K.Y.; Wu, D.Z.; Chen, H.X.; Zhang, G.Q.; Yao, R.L.; Pan, C.G.; Zhang, Z.Y. Development of low calcium fly ash-based geopolymer mortar using nanosilica and hybrid fibers. *Ceram. Int.* **2021**, *47*, 21791–21806. [[CrossRef](#)]
- Chen, K.Y.; Wu, D.Z.; Yi, M.; Cai, Q.; Zhang, Z.Y. Mechanical and durability properties of metakaolin blended with slag geopolymer mortars used for pavement repair. *Constr. Build. Mater.* **2021**, *281*, 122566. [[CrossRef](#)]

23. Chen, K.Y.; Wu, D.Z.; Zhang, Z.L.; Pan, C.G.; Shen, X.Y.; Xia, L.L.; Zang, J.W. Modeling and optimization of fly ash–slag-based geopolymer using response surface method and its application in soft soil stabilization. *Constr. Build. Mater.* **2022**, *315*, 125723. [[CrossRef](#)]
24. JGJ/T 233-2011; Specification for Mix Proportion Design of Cement Soil. China Construction Industry Press: Beijing, China, 2011.
25. Association Française de Normalisation. *Soils: Investigation and Testing—Soil Treated with Hydraulic Binder, Possible Combined with Lime, for Use as a Selected Fill Part 2: Methodology of Laboratory Formulation Studies*; Association Française de Normalisation: Paris, France, 2001.
26. ASTM D559/559M-15; Standard Test Methods for Wetting and Drying Compacted Soil-Cement Mixtures. ASTM International: West Conshohocken, PA, USA, 2015.
27. Sun, X.; Tong, Q.; Liu, W.; Yao, J.; Li, Z.Q. Study of microstructure and mechanical properties of dredged silt solidified using fly ash and slag stimulated by alkali. *J. Dalian Univ. Technol.* **2017**, *57*, 622–628.
28. Davidovits, J. Geopolymers: Inorganic polymeric new materials. *J. Therm. Anal. Calorim.* **2005**, *37*, 1633–1656. [[CrossRef](#)]
29. Bilondi, M.P.; Toufigh, M.M.; Toufigh, V. Experimental investigation of using a recycled glass powder-based geopolymer to improve the mechanical behavior of clay soils. *Constr. Build. Mater.* **2018**, *170*, 302–313. [[CrossRef](#)]
30. Shekhovtova, J.; Kearsley, E.P.; Kovtun, M. Effect of activator dosage, water-to-binder-solids ratio, temperature and duration of elevated temperature curing on the compressive strength of alkali-activated fly ash cement pastes. *J. S. Afr. Inst. Civ. Eng.* **2014**, *56*, 44–52.
31. Heah, C.Y.; Kamarudin, H.; Al Bakri, A.M.M.; Bnhussain, M.; Luqman, M.; Nizar, I.K.; Ruzaidi, C.M.; Liew, Y.M. Kaolin-based geopolymers with various NaOH concentration. *Int. J. Miner. Metall. Mater.* **2013**, *20*, 313–322. [[CrossRef](#)]
32. Cristelo, N.; Glendinning, S.; Fernandes, L.; Pinto, A.T. Effects of alkaline-activated fly ash and Portland cement on soft soil stabilisation. *Acta Geotech.* **2013**, *8*, 395–405. [[CrossRef](#)]
33. Chen, R.; Zhu, Y.; Lai, H.P.; Bao, W.X. Stabilization of soft soil using low-carbon alkali-activated binder. *Environ. Earth Sci.* **2020**, *79*, 510. [[CrossRef](#)]
34. Puligilla, S.; Mondal, P. Role of slag in microstructural development and hardening of fly ash-slag geopolymer. *Cem. Concr. Res.* **2013**, *43*, 70–80. [[CrossRef](#)]
35. Zhou, X.; Shen, J. Micromorphology and microstructure of coal fly ash and furnace bottom slag based light-weight geopolymer. *Constr. Build. Mater.* **2020**, *242*, 118168. [[CrossRef](#)]
36. Nematollahi, B.; Sanjayan, J.; Shaikh, F. Synthesis of heat and ambient cured one-part geopolymer mixes with different grades of sodium silicate. *Ceram. Int.* **2015**, *41*, 5696–5704. [[CrossRef](#)]
37. Wu, Q.S.; Li, S.Y. Research on the Preparation of Alkali-activated Cement Using the Waste Alkali Water and the Wastrel. *J. Build. Mater.* **2001**, *3*, 270–275.
38. McLellan, B.C.; Williams, R.P.; Lay, J.; van Riessen, A.; Corder, G.D. Costs and carbon emissions for geopolymer pastes in comparison to ordinary portland cement. *J. Clean. Prod.* **2011**, *19*, 1080–1090. [[CrossRef](#)]
39. Teh, S.H.; Wiedmann, T.; Castel, A.; de Burgh, J. Hybrid life cycle assessment of greenhouse gas emissions from cement, concrete and geopolymer concrete in Australia. *J. Clean. Prod.* **2017**, *152*, 312–320. [[CrossRef](#)]
40. Turner, L.K.; Collins, F.G. Carbon dioxide equivalent (CO₂-e) emissions: A comparison between geopolymer and OPC cement concrete. *Constr. Build. Mater.* **2013**, *43*, 125–130. [[CrossRef](#)]